



Cite this: DOI: 10.1039/d0dt01367f

P-Alkynyl functionalized benzazaphospholes as
transmetalating agents†Daniel Y. Zhou,^a Preston M. Miura-Akagi,^a Sierra M. McCarty,^a Celeste H. Guiles,^a
Timothy J. O'Donnell,^{id} Wesley Y. Yoshida,^a Colleen E. Krause,^b
Arnold L. Rheingold,^c Russell P. Hughes^d and Matthew F. Cain^{id} *^a

Exposure of 10 π -electron benzazaphosphole **1** to HCl, followed by nucleophilic substitution with the Grignard reagent BrMgCCPh afforded alkynyl functionalized **3** featuring an exocyclic –C≡C–Ph group with an elongated P–C bond (1.7932(19) Å). Stoichiometric experiments revealed that treatment of *trans*-Pd(PEt₃)₂(Ar)(I) (Ar = *p*-Me (**C**) or *p*-F (**D**)) with **3** generated *trans*-Pd(PEt₃)₂(Ar)(CCPh) (Ar = *p*-Me (**E**) or *p*-F (**F**)), **5**, which is the result of ligand exchange between P–I byproduct **4** and **C/D**, and the reductively eliminated product (Ar–C≡C–Ph). Cyclic voltammetry studies showed and independent investigations confirmed **4** is also susceptible to redox processes including bimetallic oxidative addition to Pd(0) to give Pd(I) dimer **6-Pd₂-(P(*t*-Bu)₃)₂** and reduction to diphosphine **7**. During catalysis, we hypothesized that this unwanted reactivity could be circumvented by employing a source of fluoride as an additive. This was demonstrated by conducting a Sonogashira-type reaction between 1-iodotoluene and **3** in the presence of 10 mol% Na₂PdCl₄, 20 mol% P(*t*-Bu)₃, and 5 equiv. of tetramethylammonium fluoride (TMAF), resulting in turnover and the isolation of Ph–C≡C–(*o*-Tol) as the major product.

Received 14th April 2020,
Accepted 16th December 2020

DOI: 10.1039/d0dt01367f

rsc.li/dalton

Introduction

Since its inception,¹ Pd-catalyzed cross coupling has evolved to a remarkable extent. Once difficult substrates like aryl chlorides (ArCl) now routinely undergo oxidative addition to Pd(0),² and Pd(Ar)(CF₃) intermediates,³ previously considered chemically inert, undergo reductive elimination when supported by an appropriate ligand.⁴ Currently, transmetalation to generate the key Pd(Ar)(R') intermediate (R' = hydrocarbyl-based group) is often a considerable challenge,⁵ especially as researchers focus on synthesizing increasingly complex and densely functionalized targets that hinge on the construction of a critical C–C bond *via* Pd-catalyzed methods.⁶ The Stille reaction,⁷ utilizing tin-based transmetalating agents, is generally considered to be the most functional group tolerant due to the low polarity of the Sn–C bond, but the high toxicity of organos-

tannanes limits its use.⁸ Despite this, numerous pharmaceutically relevant building blocks including bithiazoles⁹ and functionalized nucleosides¹⁰ are best prepared *via* Stille methodology.^{6a} We were interested in determining if transmetalating agents based on phosphorus could take advantage of the low polarity of the P–C bond without succumbing to the contamination issues that plague Sn-based reagents. Compared with the Sn–C bond, the P–C bond is stronger and significantly more inert;¹¹ however, Gudat demonstrated with 1,3,2-diazaphospholenes (**A**, also called NHPs) that the presence of adjacent sp² hybridized N atoms with lone pairs in p-type orbitals led to significant *n*(N)– σ^* (P–X) hyperconjugation and a highly polarized and reactive P–X bond.¹² In fact, it has been argued that the most important resonance contributor to 1,3,2-diazaphospholenes is ionic structure **A'** (Chart 1, top), best exempli-

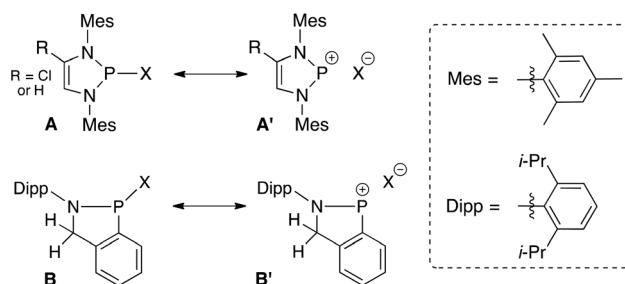


Chart 1 Relevant resonance structures for 1,3,2-diazaphospholenes (NHPs) and functionalized benzazaphospholes.

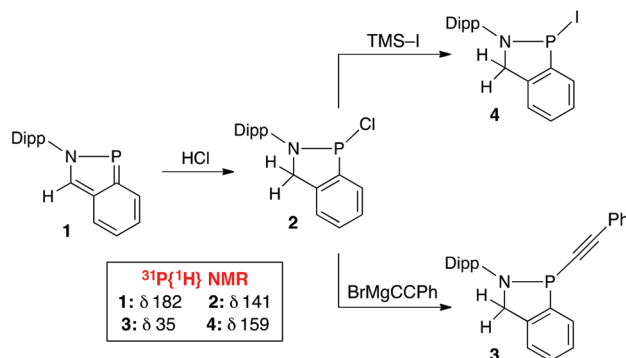
^aDepartment of Chemistry, University of Hawai'i at Mānoa, 2545 McCarthy Mall, Honolulu, Hawaii 96822, USA. E-mail: mfcain@hawaii.edu

^bDepartment of Chemistry, University of Hartford, 200 Bloomfield Avenue, West Hartford, Connecticut, 06117, USA

^cDepartment of Chemistry, University of California, San Diego, 9500 Gilman Drive, La Jolla, California 92093, USA

^d6128 Burke Laboratory, Department of Chemistry, Dartmouth College, Hanover, New Hampshire 03755, USA

† Electronic supplementary information (ESI) available. CCDC 1996894–1996896 and 2051688–2051690. For ESI and crystallographic data in CIF or other electronic format see DOI: 10.1039/d0dt01367f



Scheme 1 Syntheses of 2, 3, and 4.

fied by the room temperature transfer of the cyclopentadienyl ($X = \text{Cp}$ (C_5H_5)) anion to electrophilic Mn and Fe centers.¹³ We recently synthesized *N*-Dipp-substituted 10π -electron benzazaphospholes (**1**, see below in Scheme 1)¹⁴ and questioned if dearomatization/functionalization of the five-membered ring could afford a PN heterocycle of Type **B**, featuring a new P-X bond of enhanced polarity and reactivity (Chart 1, bottom). In order to bias the system toward ionic structure **B'**, we chose to synthesize a P-alkynyl derivative, speculating that the large degree of *s*-character (50%) in the $-\text{CCPh}$ unit would better stabilize the X^- fragment.¹⁵ Here, we report that this new P-alkynyl derivative can act as transmetalating agent in Sonogashira-type reactions.¹⁶

Results and discussion

Functionalization

Simple dearomatization/functionalization of the five-membered ring of benzazaphosphole **1** was accomplished *via* methodology similar to that reported by Nikonov.¹⁷ Specifically, exposure of **1** to two equiv. of HCl in dioxane afforded P-Cl derivative **2** in 63% yield (Scheme 1). The $^{31}\text{P}\{^1\text{H}\}$ NMR spectrum of **2** featured a single signal at 141 ppm, while ^1H NMR spectroscopy displayed the diagnostic diastereotopic CH_2 protons at 4.95 and 4.12 ppm.¹⁸ Treatment of **2** with two equiv. of the Grignard reagent $\text{BrMgC}\equiv\text{CPh}$ gave alkynyl analogue **3**.¹⁹ Starting with **1**, a streamlined and scaled up (3.69 g scale) two step sequence, bypassing the isolation of **2**, yielded 3.07 grams of **3** (62% yield). P-CCPh derivative **3** was characterized by $^{31}\text{P}\{^1\text{H}\}$, ^1H , and $^{13}\text{C}\{^1\text{H}\}$ NMR spectroscopy and elemental analysis. The structures of **2** and **3** were confirmed by X-ray crystallography (Fig. 1 and 2).

Like their NHP counterparts (see Chart 1),^{12,18} P-functionalized benzazaphospholes possess exocyclic P-X bonds that are long (for example, P-Cl bond in **2** = 2.1649(8) Å). The prevailing argument with NHPs is $n(\text{N})-\sigma^*(\text{P}-\text{X})$ hyperconjugation results in shorter P-N bonds accompanied by longer P-X bonds. Along these lines, both **2** and **3** feature P-N bond lengths slightly reduced relative to **1** (1.702 Å)²⁰ and on par with their analogous 1,3,2-diazaphospholene derivatives,

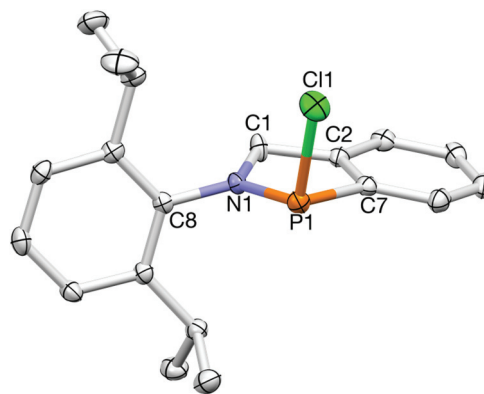


Fig. 1 X-ray crystal structure of **2**. Selected bond lengths (Å) and angles (deg): $\text{P}_1-\text{Cl}_1 = 2.1649(8)$, $\text{P}_1-\text{N}_1 = 1.6681(16)$, $\text{P}_1-\text{C}_7 = 1.818(2)$, $\text{N}_1-\text{C}_1 = 1.485(3)$, $\text{C}_1-\text{C}_2 = 1.517(3)$, $\text{N}_1-\text{P}_1-\text{Cl}_1 = 106.02(6)$, $\text{N}_1-\text{P}_1-\text{C}_7 = 89.74(9)$, $\text{C}_7-\text{P}_1-\text{Cl}_1 = 96.76(6)$.

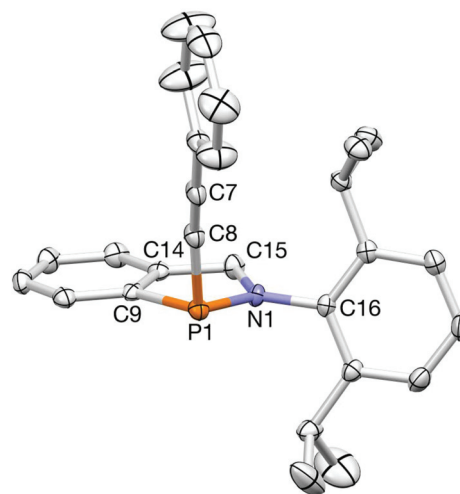


Fig. 2 X-ray crystal structure of **3**. Selected bond lengths (Å) and angles (deg): $\text{P}_1-\text{N}_1 = 1.6986(15)$, $\text{P}_1-\text{C}_9 = 1.8305(18)$, $\text{P}_1-\text{C}_8 = 1.7932(19)$, $\text{C}_9-\text{C}_{14} = 1.393(3)$, $\text{C}_{14}-\text{C}_{15} = 1.509(3)$, $\text{N}_1-\text{C}_{15} = 1.461(2)$, $\text{N}_1-\text{P}_1-\text{C}_9 = 89.64(8)$, $\text{N}_1-\text{P}_1-\text{C}_8 = 106.70(8)$, $\text{C}_8-\text{P}_1-\text{C}_9 = 99.89(8)$, $\text{P}_1-\text{C}_8-\text{C}_7 = 168.38(18)$.

but their P-X bonds are not as drastically elongated. For example, P- C_{sp} bonds in alkynylphosphines generally range from 1.728 to 1.795 Å, placing **3** (1.7932(19) Å) at the upper limit; however, 1,3,2-diazaphospholenes with $\text{X} = -\text{CCR}$ ($\text{R} = \text{H}$ or Ph) contained P-C bonds topping out at 1.827(2) Å.^{19a} Speculating the difference may originate from these heterocycles being “singly-” *versus* “doubly nitrogenated”, NBO calculations (B3LYP-D3/LACV3P**) were undertaken,²¹ revealing that both the P-Cl and P-C σ^* orbital in **2** and **3** are less occupied than their NHP analogues. The increased occupancy in NHPs resulting from more pronounced delocalization of the *N*-lone pairs, *i.e.*, $n(\text{N})-\sigma^*(\text{P}-\text{X})$ hyperconjugation, which is depicted in the NLMOs in Fig. 3, leads to significant elongation of their exocyclic P-X bonds compared with **2** and **3**. These weakened P-X bonds have been previously exploited for

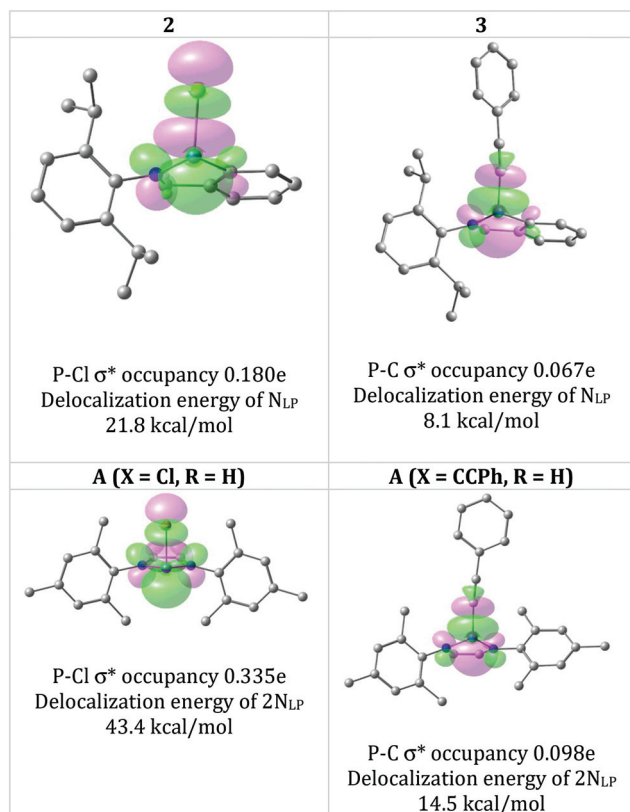


Fig. 3 Calculated NLMOs with NBO occupancies and delocalization energies for the interactions of the *N*-lone pairs of **2**, **3**, and **A** with either their P–Cl or P–C σ^* orbitals.

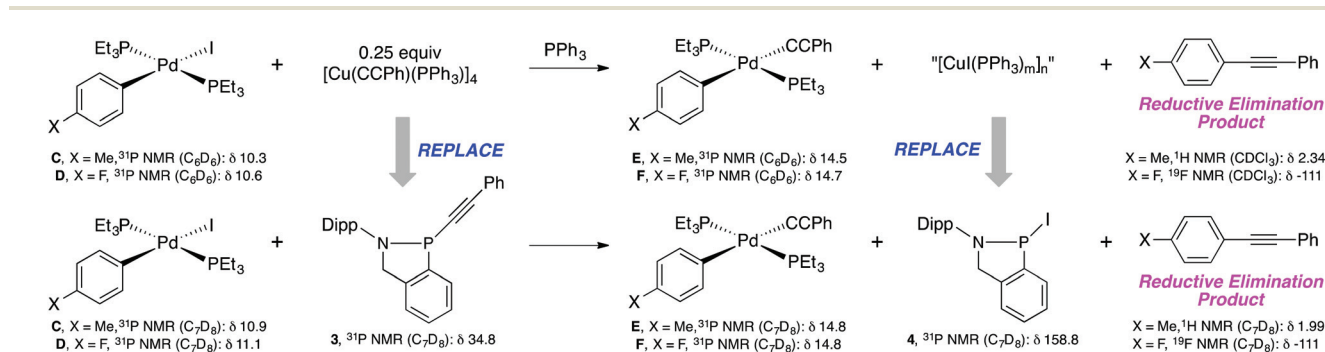
1,3,2-diazaphospholene-catalyzed P–C bond formation²² and CuCl-promoted alkynyl scrambling processes.^{19a} Despite being *less activated*, we hypothesized that the alkynyl fragment of **3** would still be susceptible to transmetalation.

Stoichiometric studies and reactivity of iodophosphine **4**

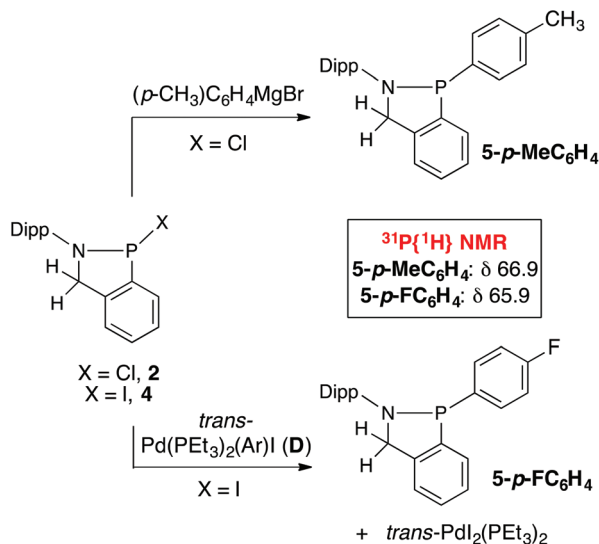
Transfer of an –CCPh unit from a Cu(I) source to an $L_nPd(Ar)$ (X) intermediate derived from the oxidative addition of an aryl halide (ArX) to a Pd(0) center to form $L_nPd(Ar)(CCPh)$ and CuX is the key step in installing the to-be-reductively-eliminated groups on the Pd(II) center in a Sonogashira reaction.²³

Previously, this transmetalation step was studied by NMR spectroscopy in a stoichiometric fashion by exposing independently prepared *trans*-Pd(PET₃)₂(Ar)(I) (Ar = *p*-MeC₆H₄ (**C**) or *p*-FC₆H₄ (**D**))²⁴ to 0.25 equiv. of tetrameric [Cu(CCPh)(PPh₃)₄] in the presence of PPh₃, resulting in the generation of *trans*-Pd(PET₃)₂(Ar)(CCPh) (Ar = *p*-MeC₆H₄ (**E**) or *p*-FC₆H₄ (**F**)), a CuI-derived triphenylphosphine complex, and the coupling product PhC≡CAr (Scheme 2, top panel).²⁵ In principle, if the [Cu(CCPh)(PPh₃)₄] species was replaced by **3**, transmetalation between the Pd–I moieties of **C/D** with the –CCPh group to give **E/F** and P–I species **4** could be easily monitored by NMR spectroscopy (Scheme 2, bottom panel).

Iodophosphine **4**, a previously unknown compound, was prepared in 71% yield as shown in Scheme 1 by treatment of P–Cl derivative **2** with TMS–I,²⁶ revealing that its ³¹P{¹H} NMR chemical shift appeared downfield at 159 ppm. The ¹H NMR spectrum (C₇D₈) featured broadened signals for the benzylic protons (δ 4.68) of the azaphosphole ring and the methine protons (δ 3.14) of the *ortho* *i*-Pr groups on the *N*-Dipp substituent. In addition, only two distinct methyl groups (rather than four like in **2** and **3**) were observed, suggesting that at room temperature **4** adopted a C_s-symmetric, ionic-type structure like **B'** (Chart 1). As the temperature was lowered below –30 °C, ¹H NMR spectroscopy showed that a C₁-symmetric, covalent structure like **B** with a *bona fide* P–I bond persisted, consistent with the appearance of diastereotopic CH₂ protons, two separate methine signals, and four methyl resonances. Ultimately, X-ray crystallography revealed that the P–I bond in **4** was elongated (2.5937(7) Å), but not severely compared with its NHP analogue (**A**, R = H, Mes groups replaced by *t*-Bu, X = I, 3.426(1) Å); see ESI† for detailed NMR spectra and X-ray structure.²⁶ Regardless, if **4** exhibited reactivity consistent with an ionic species (like **B'**) in solution, X-type ligand scrambling *via* σ -bond metathesis between the aryl group of **C/D** or **E/F** and P–I bond of **4** may occur to give *trans*-PdI₂(PET₃)₂ (³¹P NMR (CDCl₃): δ 8.4²⁷ or 8.9²⁸) or *trans*-PdI(CCPh)(PET₃)₂ (³¹P NMR (CD₂Cl₂): δ 13.9)²⁷ and **5** (Ar = *p*-MeC₆H₄ or *p*-FC₆H₄). This P–I for Pd–Ar exchange was confirmed by ³¹P{¹H} NMR spectroscopy by heating a solution of **4** and **D** in toluene at 120 °C, producing **5-p-FC₆H₄** and *trans*-PdI₂(PET₃)₂ accompanied by trace amount of **1** and presumably *trans*-Pd(PET₃)₂(*p*-FC₆H₄)₂ (Scheme 3, bottom).²⁹ Separation of the product mixture



Scheme 2 Stoichiometric transfer of –CCPh to spectroscopically characterized Pd(II) complexes.²⁵



Scheme 3 Synthetic pathways to 5.

required extraction/filtration through silica using pentane as an eluent followed by recrystallization from CH_3CN , affording $5\text{-}p\text{-FC}_6\text{H}_4$ in low yield. Independently, larger quantities of the analogous $5\text{-}p\text{-MeC}_6\text{H}_4$ were prepared by exposure of 2 to the commercially available Grignard reagent $(p\text{-CH}_3)\text{C}_6\text{H}_4\text{MgBr}$, followed by recrystallization from pentane (Scheme 3, top). Analytically pure $5\text{-}p\text{-MeC}_6\text{H}_4$ was characterized by NMR spectroscopy, elemental analysis, and X-ray crystallography (Fig. 4).

The susceptibility of 4 to redox processes was also a concern.³⁰ Cyclic voltammetry demonstrated that 4 exhibited complex redox behaviour. Across all scan rates from 25 to 1000 mV, several cathodic peaks were observed, while at low

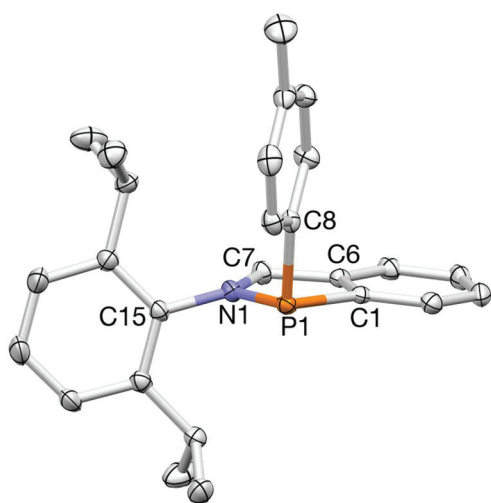


Fig. 4 X-ray crystal structure of $5\text{-}p\text{-MeC}_6\text{H}_4$. Selected bond lengths (Å) and angles (deg): $\text{P}_1\text{-C}_8 = 1.8433(13)$, $\text{P}_1\text{-N}_1 = 1.7058(11)$, $\text{P}_1\text{-C}_1 = 1.8263(13)$, $\text{N}_1\text{-C}_7 = 1.4608(16)$, $\text{N}_1\text{-C}_{15} = 1.4335(16)$, $\text{C}_1\text{-C}_6 = 1.3945(18)$, $\text{C}_6\text{-C}_7 = 1.5043(17)$, $\text{N}_1\text{-P}_1\text{-C}_1 = 89.35(5)$, $\text{N}_1\text{-P}_1\text{-C}_8 = 105.85(5)$, $\text{C}_8\text{-P}_1\text{-C}_1 = 100.44(5)$.

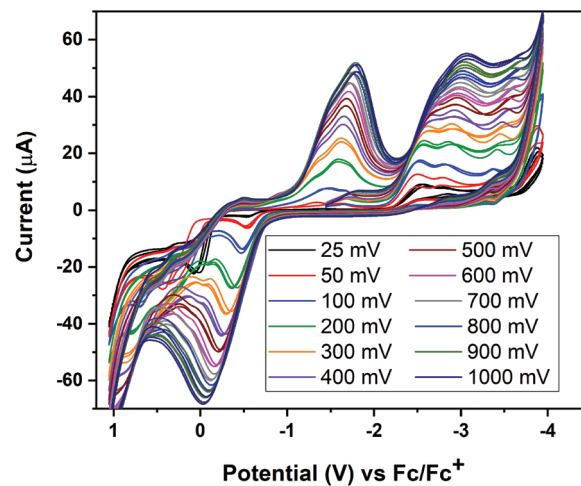
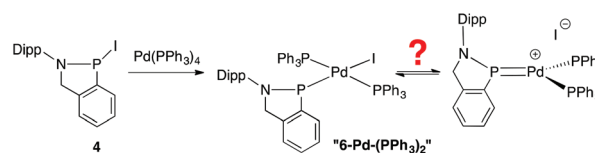


Fig. 5 An overlay of the cyclic voltammograms of 4 for scan rates varying from 25 mV to 1000 mV, referenced to the Fc/Fc^+ couple.

scan rates, two anodic peaks were detected, but coalesced into a single peak with increased scan rates. An overlay plot of the voltammograms is shown in Fig. 5.

With regard to the stoichiometric case depicted in Scheme 2, this redox “liability” of 4 may manifest itself chemically if reductive elimination from E/F is fast with respect to transmetalation, which will generate $\text{Pd}(0)$ in solution. Previously, oxidative addition between electron-rich transition metal centers like $\text{Pd}(0)$,³¹ $\text{Pt}(0)$,³² and $\text{Rh}(I)$ ³³ and NHP-X species ($\text{X} = \text{halogen}$) or their cationic analogues (NHP^+ with pseudohalogen counterion like OTf^-) has been reported with the P-center functioning as either an anionic and pyramidal phosphido (PR_2^-)³⁴ or cationic and planar phosphonium (PR_2^+) donor.^{31–33} Here, exposure of 4 to $\text{Pd}(\text{PPh}_3)_4$ produced a product mixture by $^{31}\text{P}\{^1\text{H}\}$ NMR spectroscopy, which featured a multiplet downfield at 284.5 ppm and a matching signal at 17.8 ppm, indicative of P–I activation at $\text{Pd}(0)$.^{31,32,34,35} The reduced J_{PP} coupling (30 Hz) relative to both three- ($J_{\text{PP}} = 149$ Hz)³¹ and four-coordinate ($J_{\text{PP}} = 73$ Hz)³² cationic Pd complexes of the type $[(\text{NHP})\text{Pd}(\text{PR}_3)_n][\text{OTf}]$ ($n = 2$ or 3) in which the NHP behaved as a phosphonium donor suggested that the P-center of the PN unit may be pyramidal,¹⁵ but slow decomposition prevented isolation and spectroscopic/structural characterization of tentatively assigned **6-Pd-(PPh₃)₂** (Scheme 4). Unsure of the nature of the PN donor in “**6-Pd-(PPh₃)₂**” and cognizant that the reversible halogen binding observed at $\text{Pd}(0)$ complexes derived from NHP-X species may trigger



Scheme 4 Synthesis of tentatively assigned “**6-Pd-(PPh₃)₂**” and its potential for reversible iodide binding.

unwanted ligand substitution,³¹ ion-exchange on “**6-Pd-(PPh₃)₂**” with a weakly coordinating anion was performed. However, addition of either TMSOTf or AgOTf to the reaction mixture led to rapid decomposition as observed by ³¹P{¹H} NMR spectroscopy. Attempts to selectively substitute the PPh₃ ligands with superior donors like PMe₃, PEt₃, and P(i-Pr)₃ or chelating phosphines like dppe (diphenyl(phosphine)ethane) also failed to deliver any isolable Pd complexes.³²

Fortunately, treatment of **4** with 1 equiv. of [Pd(P(*t*-Bu)₃)₂] in toluene afforded a robust Pd complex with a ³¹P{¹H} NMR spectrum featuring a triplet/doublet pattern (276.0 and 96.7 ppm, *J*_{PP} = 73 Hz) integrating in a 1 : 2 ratio (Scheme 5). Despite the prominent cone angle of P(*t*-Bu)₃,³⁶ we suspected, based on the NMR spectra of aforementioned [(NHP)Pd(PR₃)_{*n*}][OTf] (*n* = 2 or 3)^{31,32} species that **6-Pd-(P(*t*-Bu)₃)₂** was generated in solution. Recrystallization of the reaction mixture from Et₂O/CH₃CN at -35 °C afforded a dark crystalline solid with ¹H and ¹³C{¹H} NMR spectra in support of anticipated product **6-Pd-(P(*t*-Bu)₃)₂**. However, X-ray crystallography revealed and elemental analysis confirmed the structure was Pd(I)-Pd(I) dimer **6-Pd₂-(P(*t*-Bu)₃)₂** (Fig. 6). Normally,³⁷ Pd(I) dimers are formed *via* comproportionation between Pd(0) and Pd(II) precursors,³⁸ but **6-Pd₂-(P(*t*-Bu)₃)₂** is formally the product of bimetallic P-I oxidative addition to Pd(0).³⁹ Its core (see inset of Fig. 6) contains terminally bound P(*t*-Bu)₃ ligands to both Pd centers that are linked by symmetrical I and PN bridges and further supported by a Pd-Pd bond. The Pd-Pd (2.6215(3) Å), two Pd-P(*t*-Bu)₃ (2.3494(7) and 2.3467(7) Å), and two Pd-I bonds (2.7678(2) and 2.7441(2) Å), which create a severely acute Pd₁-I-Pd₂ angle of 56.795(60) deg are similar to the prototypical [Pd(P(*t*-Bu)₃)₂]₂ dimer⁴⁰ and other related⁴¹ [Pd(PR₂R')X]₂ and [Pd(NHC)X]₂ complexes.^{37,42} Akin to the Pd(I) dimer reported by Thomas featuring a symmetrically NHP-bridged diphosphine ligand,³⁴ the μ-PN donor possesses Pd-P bond lengths (Pd₁-P₁ = 2.2491(7) and Pd₂-P₁ = 2.2157(6) Å) consistent with its formulation as a bridging phosphido (μ-PR₂⁻) ligand.⁴³ By comparison, the terminally ligated NHP-phosphonium in [(NHP)Pd(PPh₃)₂][OTf]³² has a much shorter

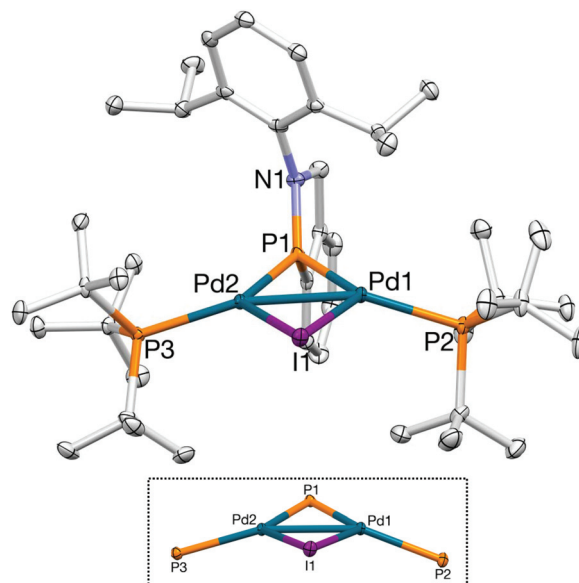
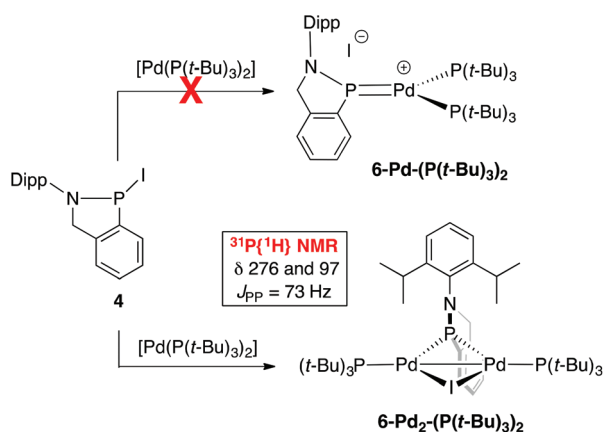


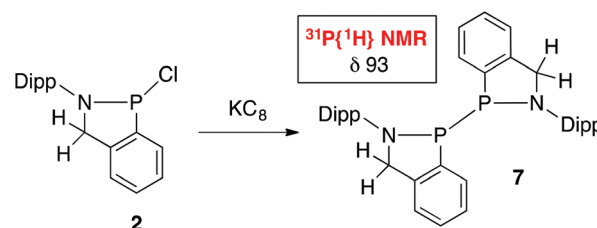
Fig. 6 X-ray crystal structure of **6-Pd₂-(P(*t*-Bu)₃)₂** with its core highlighted in the inset. Selected bond lengths (Å) and angles (deg): P₁-Pd₁ = 2.2491(7), P₁-Pd₂ = 2.2157(6), Pd₁-Pd₂ = 2.6215(3), Pd₁-P₂ = 2.3494(7), Pd₂-P₃ = 2.3467(7), Pd₁-I₁ = 2.7678(2), Pd₂-I₁ = 2.7441(2), P₁-N₁ = 1.701(2), P₁-C₁ = 1.804(2), Pd₁-P₁-Pd₂ = 71.90(2), Pd₁-I₁-Pd₂ = 56.795(6).

Pd-P bond (2.1229(11) Å) and the asymmetrically bridged analogue in [(P-(NHP)-P)Pd]₂[PF₆]₂ contains one short (2.1616(15) Å) and one long (2.4982(16) Å) Pd-P(NHP) bond.⁴⁴ With such a unique Pd₂(μ-I)(μ-PN) core, the stability of **6-Pd₂-(P(*t*-Bu)₃)₂** compared with “**6-Pd-(PPh₃)₂**” is perplexing. Further complicating matters is the unverified stoichiometric ratio of PN : Pd in “**6-Pd-(PPh₃)₂**” combined with the corresponding downfield shifted ³¹P{¹H} NMR signals (>250 ppm) of both 1 : 1 PN : Pd structures resembling [(NHP)Pd(PR₃)_{*n*}][OTf]^{31,32} or [(P-(NHP)-P)Pd]₂[PF₆]₂^{34,35,44} and 1 : 2 PN : Pd structures like **6-Pd₂-(P(*t*-Bu)₃)₂**. However, if bridging PN units and lower coordination numbers at Pd with a 1 : 2 ratio are preferred, then bulkier phosphines will be more effective at protecting the metal center from unidentified decomposition pathways like those plaguing “**6-Pd-(PPh₃)₂**”. Ultimately, an optimized protocol utilizing a 1 : 2 ratio of **4** to [Pd(P(*t*-Bu)₃)₂] afforded **6-Pd₂-(P(*t*-Bu)₃)₂** in 30% yield.

Alternatively, the P-I “bond” (*vide supra*) of **4** may be directly reduced to give diphosphine **7** (Scheme 6).^{12,30b} Initial



Scheme 5 Synthesis of **6-Pd₂-(P(*t*-Bu)₃)₂**. The fused benzene ring and carbon-containing portion of the five-membered PN ring in **6-Pd₂-(P(*t*-Bu)₃)₂** are shaded in grey to improve clarity of the structure.



Scheme 6 Synthesis of dimer **7**.

investigations with **4** using KC_8 , Mg, or alkylphosphines as reducing agents¹⁴ afforded complicated product mixtures. However, switching to P–Cl derivative **2** and KC_8 in THF was optimal, generating dimeric **7** in solution with the expected singlet observed at 93 ppm in the $^{31}\text{P}\{^1\text{H}\}$ NMR spectrum.

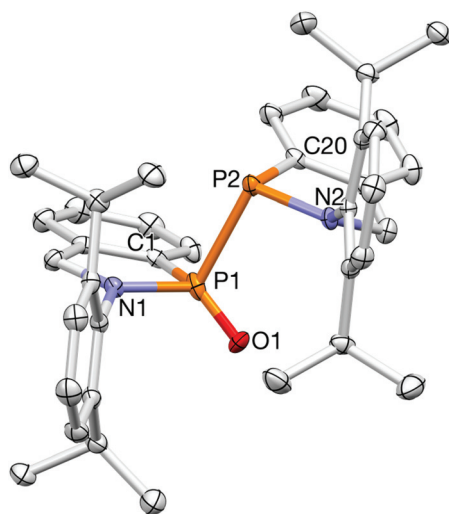


Fig. 7 X-ray crystal structure of **7(O)**.

Recrystallization from hot octane afforded **7** as an analytically pure, white crystalline solid in 43% yield.

When analyzed by ^1H NMR spectroscopy (C_6D_6), these crystals displayed diastereotopic CH_2 protons at 5.26 and 4.22 ppm; the latter signal overlapped with one of the two methine signals at 4.19 ppm, with the other resonating as a septet upfield at 3.18 ppm. In addition, four distinct methyl signals were detected. This data in combination with the $^{13}\text{C}\{^1\text{H}\}$ NMR spectrum suggested diphosphine **7** possessed two-fold symmetry in solution. However, on two separate occasions, structural confirmation of the diphosphine was complicated by oxidation in the solid state *en route* for crystallographic assignment. The structure of **7(O)** is shown in Fig. 7.

With the NMR spectroscopic signatures of the starting materials (**C/D/3**),²⁴ expected intermediates (**E/F/4**), possible side products (**5/6/7**), and products known ($\text{PhC}\equiv\text{CAr}$, $\text{Ar} = p\text{-Me}$ or -F),²⁵ the viability of **3** as a transmetalating agent was investigated (see Scheme 2, bottom panel).⁴⁵ Addition of a solution of **3** in C_7D_8 to **C** ($\text{X} = \text{Me}$, δ 10.9) followed by heating to 120 °C generated **E** ($\text{X} = \text{Me}$, δ 14.8) and **5-*p*-MeC₆H₄** as observed by $^{31}\text{P}\{^1\text{H}\}$ NMR spectroscopy, confirming our suspicion of P–I for Pd–Ar exchange (Fig. 8). The $-\text{CCPh}$ transfer was concurrently monitored by ^1H NMR spectroscopy, revealing the formation of coupled product ($\text{PhC}\equiv\text{CAr}$, $\text{Ar} = p\text{-Me}$, δ 1.99)⁴⁶ by reductive elimination from **E**. Replacement of

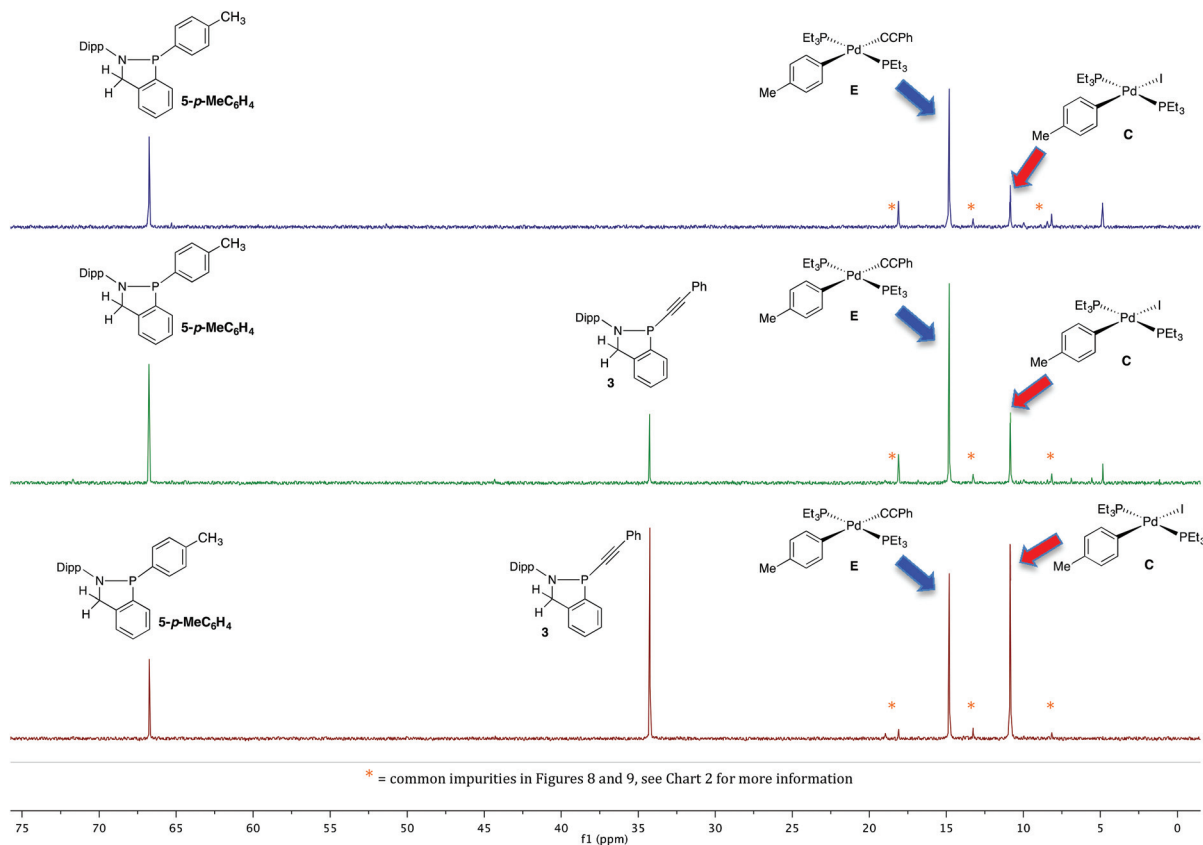


Fig. 8 Stacked $^{31}\text{P}\{^1\text{H}\}$ NMR spectra (121 MHz, C_7D_8) of the reaction progress between **C** and **3** at 12 h (bottom panel), 48 h (middle panel), and 108 h (top panel). * = common impurities in Fig. 8 and 9, see Chart 2 for more information.

methyl derivative **C** with fluorinated **D** ($X = F$) presented the opportunity to track the transmetalation with **3** by both $^{31}\text{P}\{^1\text{H}\}$ and ^{19}F NMR spectroscopy. As expected, the reaction progress between **D** and **3** at 120°C was remarkably similar to the analogous reaction with **C** by $^{31}\text{P}\{^1\text{H}\}$ NMR spectroscopy, producing **F** ($X = F$, δ 14.8) and **5-*p*-FC₆H₄** (Fig. 9); in neither case was a ^{31}P signal corresponding to P-I species **4** detected. However, ^{19}F NMR spectroscopy enabled the simultaneous observation of starting material **D** (δ -121.7), intermediate **F** (δ -122.3), and fluorine-containing product $\text{PhC}\equiv\text{C}\text{Ar}$ ($\text{Ar} = p\text{-F}$, δ -111), which coincidentally has an overlapping signal with **5-*p*-FC₆H₄** (δ -111, Fig. 10). Fig. 8–10 show the reaction between **C/D** and **3** at low, middle, and >95% conversion (for **C** + **3** = 108 h, for **D** + **3** = 120 h), respectively.

The common phosphorus-containing impurities observed by NMR spectroscopy in Fig. 8 and 9 (see Chart 2 for their structures and $^{31}\text{P}\{^1\text{H}\}$ NMR signals) also reveal the compounding effect of the side reaction between **4** and **D** (or **C**) documented in Scheme 3 to give **5-*p*-FC₆H₄** (or **5-*p*-MeC₆H₄**) and *trans*-PdI₂(PEt₃)₂.^{27,28} Subsequent mono- and dialkynylation of *trans*-PdI₂(PEt₃)₂ by **3** gives *trans*-PdI(CCPh)(PEt₃)₂ and *trans*-Pd(CCPh)₂(PEt₃)₂, both of which were detected in the stoichiometric experiments by $^{31}\text{P}\{^1\text{H}\}$ NMR spectroscopy (see Fig. 8 and 9).^{27,47} If a similar sequence were to occur after a single turnover during catalysis, *i.e.*, P-I/Pd-Ar exchange fol-

lowed by dialkynylation with **3**, then a $L_n\text{Pd}(\text{CCPh})_2$ intermediate would be generated. Reductive elimination would produce the diyne $\text{Ph-C}\equiv\text{C-C}\equiv\text{C-Ph}$,⁴⁸ a well documented side product in Sonogashira reactions that may be even more prevalent here. In order to combat this potential problem, an effective method of siphoning **4** away from the catalytic cycle was needed.

Preliminary catalytic performance

First though, a published Sonogashira reaction requiring a Cu(I)-based transmetalating agent⁴⁹ was selected as a model (Scheme 7, left).⁵⁰ At the onset, the aryl bromide substrate was replaced with the analogous aryl iodide because transmetalation of the -CCPh group was established for Pd-I species, but not the corresponding bromide. The loading of [Pd] and phosphine was increased to 10 and 20%, respectively, and the Cu(I) source and substituted acetylene were replaced by **3**. However, this preliminary trial only afforded trace coupled product ($\text{Ph-C}\equiv\text{C-(}o\text{-Tol)}$) as observed by NMR spectroscopy (diagnostic signals: ^1H (CDCl₃): δ 2.59; $^{13}\text{C}\{^1\text{H}\}$: δ 93.3 and 88.3).⁵¹ Given no diyne was detected ($\text{Ph-C}\equiv\text{C-C}\equiv\text{C-Ph}$, diagnostic signals: $^{13}\text{C}\{^1\text{H}\}$ (CDCl₃): δ 81.5 and 73.9),⁴⁸ most likely a reaction reminiscent of that shown in Scheme 5 between P-I byproduct **4** and Pd(0) resulted in the poisoning of the active catalyst after a single turnover. Thus, a source of fluoride, previously recog-

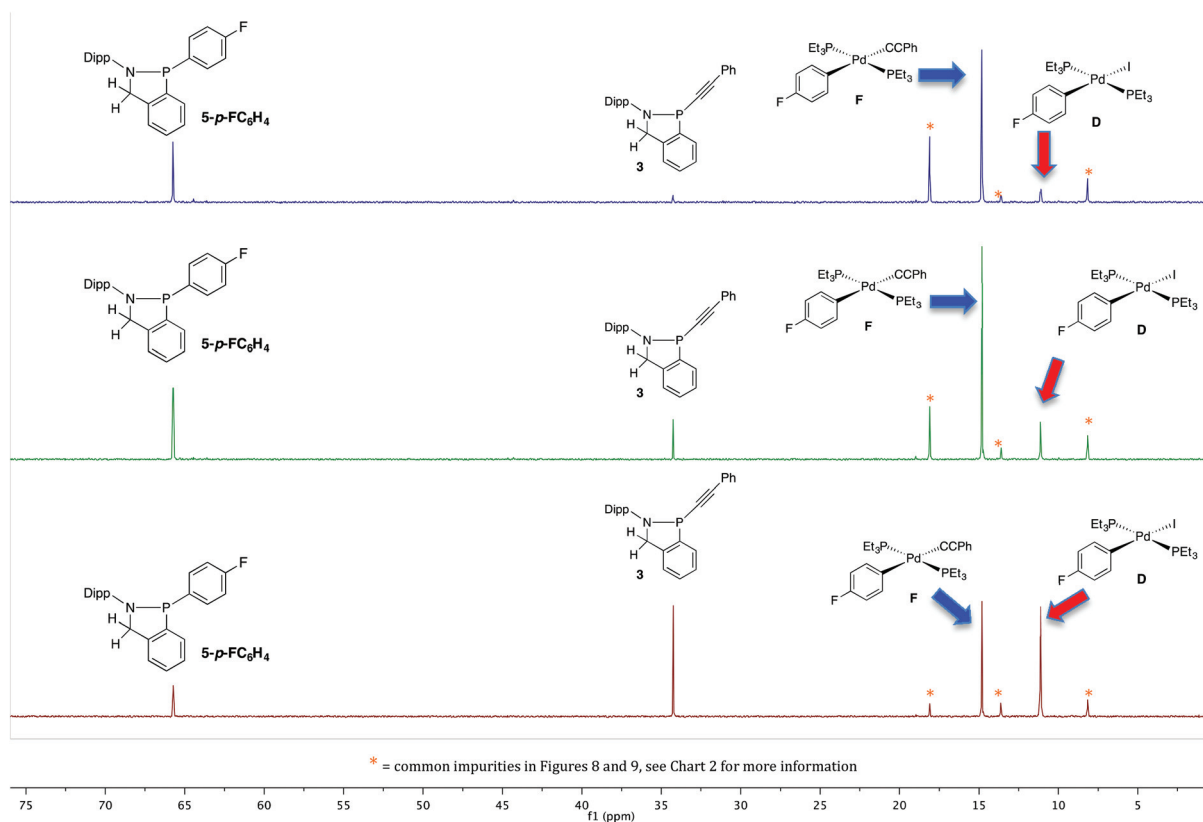


Fig. 9 Stacked $^{31}\text{P}\{^1\text{H}\}$ NMR spectra (121 MHz, C_7D_8) of the reaction progress between **D** and **3** at 12 h (bottom panel), 60 h (middle panel), and 120 h (top panel). * = common impurities in Fig. 8 and 9, see Chart 2 for more information.

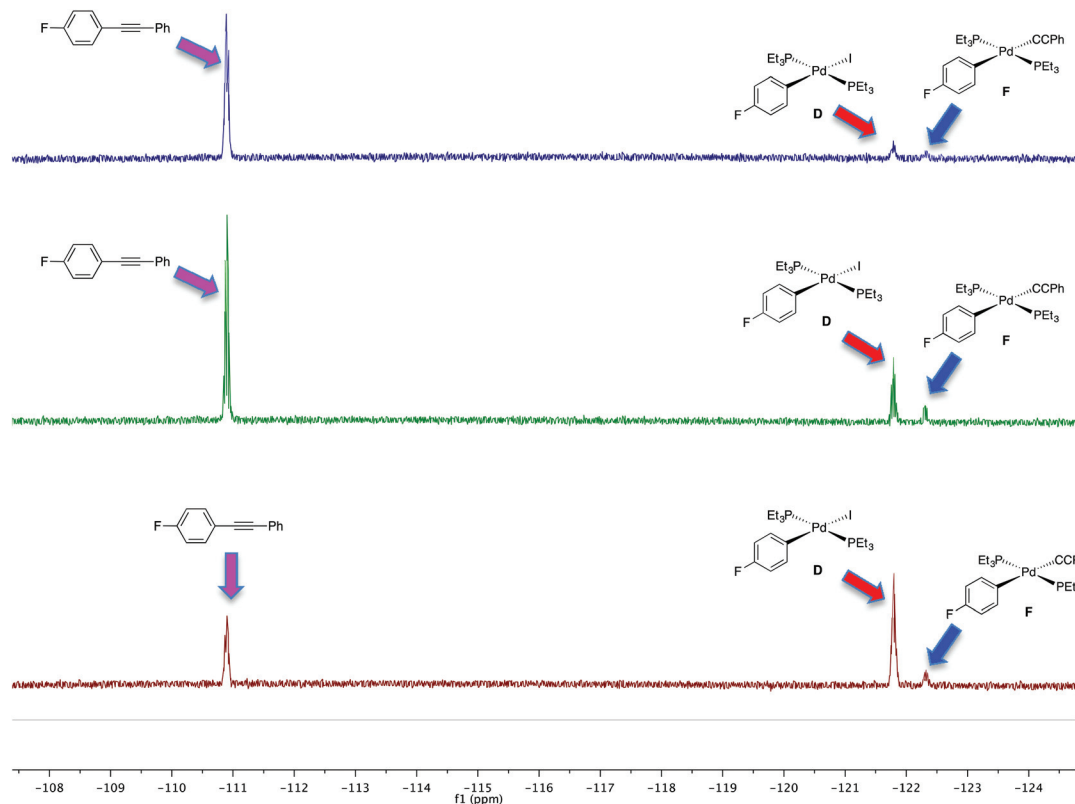


Fig. 10 Stacked ^{19}F NMR spectra (282 MHz, C_7D_8) of the reaction progress between D and 3 at 12 h (bottom panel), 60 h (middle panel), and 120 h (top panel).

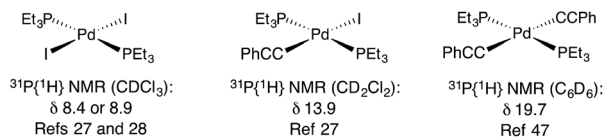
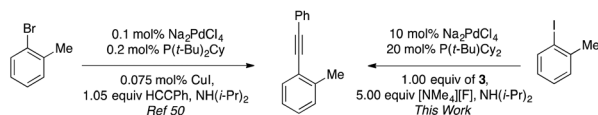


Chart 2 Impurities identified by $^{31}\text{P}\{^1\text{H}\}$ NMR spectroscopy in Fig. 8 and 9 during the stoichiometric transfer of $-\text{CPh}$ to Pd(II).



Scheme 7 Previously published sonogashira reaction (left) compared with a modified prep using benzazaphosphole-derived transmetalating agent 3 (right).

nized as an effective activating agent in Pd-catalyzed Hiyama couplings⁵² and recently discovered to transform iodophosphine 4 into the corresponding fluorophosphine,⁵³ was tested as a means of removing 4 from the catalytic cycle. Indeed, the use of CsF (5 equiv.) as an additive enabled some turnover with no diyne side product ($\text{Ph}-\text{C}\equiv\text{C}-\text{C}\equiv\text{C}-\text{Ph}$) detected by NMR spectroscopy, suggesting under the catalytic conditions fluoride reacted faster with 4 than Pd(0) or any P-I/Pd-Ar exchange process.

Control experiments confirmed that:

1. In the absence of Na_2PdCl_4 , phosphine, and CsF, no coupled products or obvious decomposition was detected by NMR spectroscopy when 1-iodotoluene and 3 were heated in $\text{NH}(\text{i-Pr})_2$.
2. Exposure of 1-iodotoluene and 3 to CsF did not generate the targeted substituted acetylene.
3. Replacement of 3 by phenylacetylene in the absence of CsF, conditions mimicking protonation of 3 by trace water accompanied by activation/deprotonation (with $\text{NH}(\text{i-Pr})_2$)/transmetalation of the alkyne solely by Pd(II),⁴⁹ did produce a minor amount of product. However, this is unlikely to be an operable pathway during catalysis because control experiment 1 demonstrated that prolonged exposure of a solution of 3 in $\text{NH}(\text{i-Pr})_2$ to heat does not produce phenylacetylene *via* either σ -bond metathesis or reaction with adventitious water.

Ultimately, after brief screening of ligand/additive combinations (Scheme 7, right), it was demonstrated that $\text{P}(\text{t-Bu})\text{Cy}_2/[\text{NMe}_4][\text{F}]$ (TMAF, tetramethylammonium fluoride, 5 equiv.) performed best and the coupled product could readily be separated from the reaction mixture by flash chromatography (pentane).⁵⁰ However, $\text{Ph}-\text{C}\equiv\text{C}-(\text{o-Tol})$ was isolated in only 27% yield, indicative of a catalytic process that shuts down after ~ 3 turnovers. More extensive investigation into the reactions conditions (solvents, Pd precursors, ligands, *etc.*) including additives (fluoride sources or others) combined with sys-

tematic modification of the benzazaphosphole framework (*N*-substituent effects, *etc.*) will be required to make **3** (or its derivatives) a viable option as a transmetalation agent for Pd-catalyzed cross-coupling reactions.

Conclusions

This report demonstrates for the first time that phosphorus-based compounds can act as transmetalating agents in Pd-catalyzed cross-coupling reactions. Stoichiometric studies revealed that exchange of iodide in *trans*-Pd(PET₃)₂(Ar)(I) (**C/D**) for the P-CCPh unit in **3** afforded Pd(PET₃)₂(Ar)(CCPh) (**E/F**), coupled product (PhCCAr), and **5-*p*-(Me/F)C₆H₄**, derived from a secondary reaction of P-I byproduct **4** with **C/D**. Furthermore, a catalytic variant was established with its success hinging on the use of a fluoride source to sequester **4**. Future investigations will focus on addressing the two most glaring limitations of this methodology:

1. The high temperature required to promote transmetalation between **3** and Pd(II) and
2. The low catalytic yield, which is likely linked to discovering an additive that will efficiently remove P-I byproduct **4** without jeopardizing any of the other steps in catalysis.

Experimental section

General experimental details

Unless otherwise specified, all reactions and manipulations were performed under a nitrogen atmosphere in a MBraun glovebox or using standard Schlenk techniques. All glassware was oven-dried overnight (at minimum) at 140 °C prior to use. Anhydrous solvents were purchased directly from chemical suppliers (Aldrich or Acros), pumped directly into the glove box, and stored over oven-activated 4 or 5 Å molecular sieves (Aldrich). 4N HCl in dioxane, TMS-I, BrMgCCPh, Na₂PdCl₄, P(*t*-Bu)₂Cy, P(*t*-Bu)Cy₂, PCy₃, CuI, and anhydrous NH(*i*-Pr)₂ were purchased from commercial suppliers. Benzazaphosphole **1** and Pd(II) complexes **C** and **D** were prepared by the published methods.^{14a,24} NMR spectra were obtained on either Varian spectrometers operating at 300, 400, or 500 MHz; all spectra are displayed in the ESI.† NMR chemical shifts are reported as ppm relative to tetramethylsilane and are referenced to the residual proton or ¹³C signal of the solvent (¹H CDCl₃, 7.27 ppm; ¹H C₆D₆, 7.16 ppm; ¹³C CDCl₃ 77.16 ppm; ¹³C C₆D₆, 128.06 ppm).

Synthesis of **2**

Compound **1** (100 mg, 0.339 mmol) was dissolved in 3 mL of toluene in a Schlenk bomb in the glovebox. The solution was taken out of the glovebox and 4N HCl in dioxane (169 μL, 0.678 mmol, 2 equiv.) was injected *via* syringe under positive N₂ pressure and stirred for 15 min. The reaction mixture was concentrated under vacuum, and the residual yellow solid was recrystallized from 10 mL of a 1:1 mixture of CHCl₃ and

MeCN at −35 °C to give a white solid **2** (70 mg, 0.211 mmol, 63%). Crystals suitable for X-ray diffraction were obtained from this recrystallization.

Anal. calcd for C₁₉H₂₃ClNP: C, 68.77; H, 6.99; N, 4.22. Found: C, 68.67; H, 6.98; N, 4.08. ³¹P{¹H} NMR (202 MHz, C₆D₆): δ 141.0. ¹H NMR (500 MHz, C₆D₆): δ 7.64 (m, 1H, Ar), 7.15 (m, 3H, Ar), 7.04 (m, 2H, Ar), 6.89 (m, 1H, Ar), 4.95 (dd, *J* = 18, 6 Hz, 1H, CH₂), 4.12 (dd, *J* = 18, 6 Hz, 1H, CH₂), 3.78 (sept, *J* = 6 Hz, 1H, CH), 2.74 (sept, *J* = 6 Hz, 1H, CH), 1.42 (d, *J* = 6 Hz, 3H, Me), 1.19 (d, *J* = 6 Hz, 3H, Me), 1.11 (d, *J* = 6 Hz, 3H, Me), 0.9 (d, *J* = 6 Hz, 3H, Me). ¹³C NMR (125 MHz, C₆D₆): δ 149.1 (d, *J* = 4 Hz, Ar), 147.0 (d, *J* = 4 Hz, Ar), 143.9 (Ar), 143.6 (d, *J* = 21 Hz, Ar), 136.8 (d, *J* = 13 Hz, Ar), 130.3 (Ar), 128.5 (Ar), 128.3 (d, *J* = 5 Hz, Ar), 128.1 (d, *J* = 7 Hz, Ar), 124.5 (Ar), 124.2 (Ar), 122.4 (Ar), 64.1 (d, *J* = 16 Hz, CH₂), 28.5 (CH), 28.4 (CH), 25.17 (Me), 25.13 (Me), 24.9 (d, *J* = 5 Hz, Me), 24.7 (Me).

Synthesis of **3**

Compound **1** (3.69 g, 12.5 mmol) and a stir bar were loaded in a Schlenk bomb inside the glovebox and dissolved in 10 mL of toluene. The bomb was taken outside the glovebox and HCl (4 N in 1,4-dioxane, 6.25 mL, 25.0 mmol, 2.00 equiv.) was injected through a septum *via* syringe under positive N₂ pressure. The mixture was stirred at room temperature for 15 min. The bomb was brought back into the glovebox, and the reaction mixture was concentrated under vacuum. The residue was washed with 10 mL of pentane, re-concentrated, and then dissolved in 10 mL of THF. The bomb was taken back outside the glovebox and placed in an ice bath at 0 °C and BrMgCCPh (1.0 M in THF, 25.0 mL, 25.0 mmol, 2.00 equiv.) was injected through a septum *via* syringe under positive N₂ pressure. The reaction mixture was warmed to room temperature overnight and then concentrated under vacuum on the Schlenk line. The residue was brought back inside the glovebox and extracted with pentane and filtered through Celite. The filtrate was concentrated to 50 mL and put in the freezer at −35 °C, resulting in the precipitation of the product as a white crystalline solid (3.07 g, 7.72 mmol, 62%). Redissolving a portion of the crystalline product in pentane, followed by subsequent cooling to −35 °C afforded X-ray quality crystals.

Anal. calcd for C₂₇H₂₈NP: C, 81.58; H, 7.10; N, 3.52. Found: C, 81.09; H, 6.97; N, 3.23. ³¹P{¹H} NMR (160 MHz, C₆D₆): δ 34.8. ¹H NMR (500 MHz, CDCl₃): δ 7.82–7.75 (m, 1H, Ar), 7.49–7.36 (m, 5H, Ar), 7.34–7.26 (m, 4H, Ar), 7.24–7.18 (m, 2H, Ar), 5.12 (d, *J* = 15 Hz, 1H, CH₂), 4.35 (dd, *J* = 14, 14 Hz, 1H, CH₂), 3.86 (septet, *J* = 7 Hz, 1H, CH), 2.88 (septet, *J* = 7 Hz, 1H, CH), 1.31 (d, *J* = 7 Hz, 6H, Me), 1.24 (d, *J* = 7 Hz, 3H, Me), 1.12 (d, *J* = 7 Hz, 3H, Me). ¹³C{¹H} NMR (125 MHz, CDCl₃): δ 150.7 (Ar), 148.1 (Ar), 144.3 (Ar), 139.9 (d, *J* = 16 Hz, Ar), 139.7 (d, *J* = 10 Hz, Ar), 131.6 (Ar), 128.6 (d, *J* = 19 Hz, Ar), 128.2 (Ar), 127.9 (Ar), 127.6 (d, *J* = 7 Hz, Ar), 127.5 (Ar), 127.3 (Ar), 124.2 (Ar), 123.8 (Ar), 122.9 (Ar), 122.4 (Ar), 104.8 (d, *J* = 11 Hz, P–C≡C), 92.0 (d, *J* = 77 Hz, P–C≡C), 62.8 (d, *J* = 11 Hz, CH₂), 28.8 (CH), 28.4 (CH), 25.4 (Me), 25.1 (Me), 24.7 (Me), 24.6 (Me).

Synthesis of **4**

Compound **1** (0.250 g, 0.85 mmol) and a stir bar were loaded in a Schlenk bomb inside the glovebox and dissolved in 10 mL of toluene. The bomb was taken outside the glovebox and HCl (4 N in 1,4-dioxane, 0.425 mL, 1.7 mmol, 2.00 equiv.) was injected through a septum *via* syringe under positive N₂ pressure. The mixture was stirred at room temperature for 15 min. The bomb was brought back into the glovebox and the reaction mixture was concentrated under vacuum. The residue was then dissolved in 10 mL of DCM, TMS-I (0.186 g, 0.93 mmol, 1.1 equiv.) was added dropwise, and the reaction mixture was stirred overnight then concentrated. The crude solid was recrystallized from a 2 : 1 mixture of Et₂O/pentane at -35 °C, resulting in the precipitation of the product as a yellow crystalline solid (0.253 g, 0.60 mmol, 71%).

Anal. calcd for C₂₇H₂₈NP: C, 53.91; H, 5.48; N, 3.31. Found: C, 54.33; H, 5.56; N, 3.17. ³¹P{¹H} NMR (160 MHz, C₇D₈): δ 158.8. ¹H NMR (500 MHz, CDCl₃): δ 7.96 (dd, *J* = 7, 3.5 Hz, 1H, Ar), 7.54–7.43 (m, 4H, Ar), 7.36–7.33 (m, 1H, Ar), 7.26–7.20 (m, 1H, Ar), 4.68 (br, 2H, CH₂), 3.14 (br, 2H, CH), 1.30 (d, *J* = 6 Hz, 6H, Me), 1.19 (d, *J* = 6 Hz, 6H, CH₃). ¹³C{¹H} NMR (125 MHz, CDCl₃): δ 157.8 (Ar), 143.9 (Ar), 143.0 (d, *J* = 28 Hz, Ar), 136.4 (d, *J* = 12 Hz, Ar), 130.1 (Ar), 128.6 (Ar), 128.2 (Ar), 128.1 (d, *J* = 20 Hz, Ar), 124.7 (Ar), 122.3 (Ar), 65.2 (d, *J* = 17 Hz, CH₂), 28.5 (Me), 25.1 (overlapping CH and Me).

Synthesis of 5-*p*-MeC₆H₄

Compound **1** (200 mg, 0.677 mmol) and a stir bar were loaded in a Schlenk bomb inside the glovebox and dissolved in 4 mL of toluene. The bomb was taken outside of the glovebox and HCl (4 N in 1,4-dioxane, 340 μL, 1.35 mmol, 2.00 equiv.) was injected through a septum *via* syringe under positive N₂ pressure. The mixture was stirred at room temperature for 15 min. The bomb was brought back into the glovebox, and the reaction mixture was concentrated under vacuum. The residue was washed with 5 mL of pentane, re-concentrated, and then dissolved in 5 mL of THF. The bomb was taken back outside the glovebox and placed in an ice bath at 0 °C and (*p*-Me)C₆H₄MgBr (1.0 M in THF, 1.35 mL, 1.35 mmol, 2.00 equiv.) was injected through a septum *via* syringe under positive N₂ pressure. The reaction mixture was warmed to room temperature over the course of 30 min and then brought back inside the glovebox and concentrated under vacuum. The residue was suspended in 5 mL of pentane, filtered through a Celite plug, and then washed with an additional 5 mL of pentane. The filtrates were combined and concentrated to ~5 mL and put in the freezer at -35 °C, resulting in the precipitation of the product as a white crystalline solid (89 mg, 0.230 mmol, 34%). Dissolving 10 mg of this solid in 3 mL of acetonitrile, followed by subsequent cooling to -35 °C afforded X-ray quality crystals.

Anal. calcd for C₂₆H₃₀NP: C, 80.59; H, 7.80; N, 3.61. Found: C, 80.25; H, 7.78; N, 3.73. ³¹P{¹H} NMR (160 MHz, CDCl₃): δ 66.9. ¹H NMR (500 MHz, CDCl₃): δ 7.49–7.33 (m, 4H, Ar), 7.23–7.14 (m, 4H, Ar), 7.06–7.00 (m, 3H, Ar), 5.13 (d, *J* = 15 Hz,

1H, CH₂), 4.38 (dd, *J* = 15, 10 Hz, 1H, CH₂), 2.98 (septet, *J* = 7 Hz, 1H, CH), 2.92 (septet, *J* = 7 Hz, 1H, CH), 2.30 (3H, Me), 1.30 (d, *J* = 7 Hz, 3H, Me), 1.10 (d, *J* = 7 Hz, 3H, Me), 1.04 (d, *J* = 7 Hz, 3H, Me), 0.47 (d, *J* = 7 Hz, 3H, Me). ¹³C{¹H} NMR (125 MHz, CDCl₃): δ 150.3 (Ar), 148.4 (Ar), 144.2 (Ar), 142.4 (Ar), 141.2 (d, *J* = 17 Hz, Ar), 140.7 (d, *J* = 40 Hz, Ar), 139.7 (Ar), 132.8 (d, *J* = 23 Hz), 128.8 (d, *J* = 7 Hz, Ar), 128.5 (d, *J* = 25 Hz, Ar), 128.2 (Ar), 127.4 (d, *J* = 8 Hz, Ar), 126.8 (Ar), 124.4 (Ar), 123.5 (Ar), 122.2 (Ar), 63.5 (d, *J* = 10 Hz, CH₂), 28.3 (d, *J* = 6 Hz, CH), 28.2 (CH), 25.0 (Me), 24.7 (Me), 24.6 (Me), 23.8 (Me), 21.4 (Me).

Generation of 5-*p*-FC₆H₄

Compounds **4** (58 mg, 0.137 mmol) and **D** (78 mg, 0.137 mmol) were combined in a vial, dissolved in 5 mL of toluene, and transferred to a Schlenk bomb inside the glovebox. The bomb was taken outside the glovebox and placed in an oil bath at 120 °C. After 24 h, ³¹P{¹H} NMR spectroscopy revealed the formation of 5-*p*-FC₆H₄ (65.6 ppm) and *trans*-PdI₂(PEt₃)₂ (8.0 ppm) as the major products accompanied by a trace amount of **1** (182.2 ppm) and presumably *trans*-Pd(*p*-FC₆H₄)₂(PEt₃)₂ (16.7 ppm).²⁹ The reaction mixture was subsequently brought back inside the glovebox and concentrated under vacuum. The crude product mixture was recrystallized from CH₃CN, which removed **1** and *trans*-Pd(*p*-FC₆H₄)₂(PEt₃)₂. Dissolving the remaining two components of the precipitate in 1 mL of pentane followed by filtration through a silica plug, followed by further elution with 2–3 mL of pentane afforded a filtrate with only a single ³¹P NMR (121 MHz, CDCl₃) signal (65.9 ppm). Concentration of the filtrate under vacuum afforded 7 mg of a slightly impure white solid by ¹H and ¹³C{¹H} NMR spectroscopy. Diagnostic ¹H NMR (500 MHz, CDCl₃): δ 5.12 (d, *J* = 15 Hz, 1H, CH₂), 4.38 (dd, *J* = 15, 15 Hz, 1H, CH₂), 2.95 (septet, *J* = 7 Hz, 1H, CH), 2.87 (septet, *J* = 7 Hz, 1H, CH).

Synthesis of 6-Pd₂-(*P*(*t*-Bu)₃)₂

1 : 1 stoichiometry. Compound **4** (50 mg, 0.118 mmol), [Pd(*P*(*t*-Bu)₃)₂] (60 mg, 0.118 mmol), and a stir bar were combined in a vial and dissolved in 3 mL of toluene, resulting in a dark reaction mixture. After 24 h at room temperature, ³¹P{¹H} NMR spectroscopy revealed that **4** had been consumed. The reaction mixture was subsequently concentrated under vacuum, and the dark residue was extracted with pentane (2 × 5 mL) and filtered through a Celite plug. The filtrate was concentrated under vacuum and re-dissolved in 2 mL of ether, followed by the addition of 4 mL of acetonitrile. The Et₂O/CH₃CN solution was then cooled to -35 °C, leading to the precipitation of dark crystals suitable for X-ray diffraction (<10 mg).

1 : 2 stoichiometry. Compound **4** (31 mg, 0.0732 mmol), [Pd(*P*(*t*-Bu)₃)₂] (75 mg, 0.147 mmol, 2 equiv.), and a stir bar were combined in a vial and dissolved in 3 mL of toluene, resulting in a dark reaction mixture. After 24 h at room temperature, ³¹P{¹H} NMR spectroscopy revealed that **4** had been consumed. The reaction mixture was concentrated under vacuum, pentane was added, and the mixture was re-concentrated.

Extraction of the dark residue with additional pentane (3 × 5 mL) followed by filtration through a Celite plug afforded a dark filtrate that was concentrated under vacuum. The crude product mixture was dissolved in 2 mL of ether, 4 mL of acetonitrile was added, and the solution was cooled to −35 °C, resulting in the precipitation of a dark crystalline solid. In order to remove an unidentified impurity (³¹P NMR (C₆D₆): 84.7 ppm) that was not present in the 1 : 1 stoichiometric case, the crystalline solid was washed with cold pentane, affording analytically pure material (23 mg, 0.0220 mmol, 30%).

Anal. calcd for C₄₃H₇₇INP₃Pd₂: C, 49.62; H, 7.46; N, 1.35. Found: C, 49.60; H, 7.51; N, 1.32. ³¹P{¹H} NMR (160 MHz, C₆D₆): δ 275.8 (t, *J* = 73 Hz, PN), 96.5 (d, *J* = 73 Hz, P(*t*-Bu)₃). ¹H NMR (500 MHz, C₆D₆): δ 7.90 (t, *J* = 7 Hz, 1H, Ar), 7.14–7.06 (br m, 5H, overlapping Ar), 6.96 (d, *J* = 7 Hz, 1H, Ar), 4.46 (br, 2H, CH₂), 3.85 (septet, *J* = 7 Hz, 2H, CH), 1.45 (br, 6H, Me), 1.30 (br m, 60H, overlapping *t*-Bu and Me). ¹³C{¹H} NMR (125 MHz, C₆D₆): δ 147.1 (Ar), 146.4 (Ar), 140.4 (Ar), 139.7 (Ar), 129.2 (d, *J* = 24 Hz, Ar), 128.8 (Ar), 127.4 (d, *J* = 11 Hz, Ar), 126.8 (Ar), 125.3 (Ar), 122.3 (Ar), 63.9 (CH₂), 36.5 (quat), 32.8 (*t*-Bu), 29.0 (CH), 27.9 (Me), 25.6 (Me).

Synthesis of 7

Compound **1** (200 mg, 0.68 mmol) and a stir bar were loaded in a Schlenk bomb inside the glovebox and dissolved in 5 mL of toluene. The bomb was taken outside the glovebox and HCl (4 N in 1,4-dioxane, 0.34 mL, 1.36 mmol, 2.00 equiv.) was injected through a septum *via* syringe under positive N₂ pressure. The reaction mixture was stirred at room temperature for 15 min. The bomb was then brought back into the glovebox, and the reaction mixture was concentrated under vacuum. The residue was washed with 10 mL of pentane, concentrated under vacuum, and then dissolved in 10 mL of THF. Solid K₂CO₃ (0.100 g, 0.74 mmol, 1.1 equiv.) was added, and the reaction mixture was stirred overnight. The heterogeneous mixture was concentrated under vacuum, extracted with pentane, and filtered through a Celite plug. The filtrate was transferred to a 25 mL Schlenk bomb and concentrated again. Anhydrous octane (10 mL) was added to give a slurry and the Schlenk bomb was taken outside the glovebox. The slurry was heated at 70 °C until it became homogenous. The solution was then cooled to room temperature, resulting in the precipitation of white X-ray quality crystals (87 mg, 0.15 mmol, 43%).

Anal. calcd for C₃₈H₄₆N₂P₂: C, 77.00; H, 7.82; N, 4.73. Found: C, 76.96; H, 8.09; N, 4.44. ³¹P{¹H} NMR (160 MHz, CDCl₃): δ 93.3. ¹H NMR (500 MHz, C₆D₆): δ 7.15–7.13 (m, 2H, Ar), 7.11–6.98 (m, 6H, Ar), 6.90–6.85 (m, 4H, Ar), 6.61 (d, *J* = 7.5 Hz, 2H, Ar), 5.26 (d, *J* = 15 Hz, 2H, CH₂), 4.24–4.15 (overlapping m, 4H, overlapping CH w/diastereotopic CH₂), 3.18 (septet, *J* = 7 Hz, 2H, CH), 1.36 (d, *J* = 7 Hz, 6H, CH₃), 1.26 (d, *J* = 7 Hz, 6H, CH₃), 0.94 (d, *J* = 7 Hz, 6H, CH₃), 0.79 (d, *J* = 7 Hz, 6H, CH₃). ¹³C{¹H} NMR (125 MHz, C₆D₆): δ 150.3 (Ar), 148.3 (Ar), 144.7 (Ar), 129.9 (t, *J* = 13 Hz, Ar), 127.4 (Ar), 126.5 (Ar), 124.8 (Ar), 124.1 (Ar), 121.2 (Ar), 64.6 (CH₂), 29.0 (CH), 28.8 (CH), 26.1 (Me), 25.2 (Me), 24.6 (Me), 23.3 (Me). Once isolated, diphosphine **7** routinely decomposed in solution. In CDCl₃,

the decomposition was fast, but even in C₆D₆, slow decomposition was apparent as evidenced by the appearance of other diastereotopic-type CH₂ and *N*-Dipp methyl signals. The ¹³C{¹H} NMR spectrum has fewer than the expected amount of Ar resonances likely due to overlap with the residual solvent signal.

Stoichiometric studies

Alkynyl-functionalized benzazaphosphole **3** (25 mg, 0.063 mmol) was dissolved in approximately 1.5 mL of C₇D₈ and added to Pd complex **C** or **D** (35 mg, 0.063 mol). The reaction mixture was transferred to a J-Young tube and placed in an oil bath at 120 °C. The reaction was monitored by ¹H and ³¹P{¹H} for **C** and ³¹P{¹H} and ¹⁹F NMR spectroscopy for **D** in 12 h intervals until >95% conversion was reached. See the ESI† for all NMR spectra.

Catalytic studies

Na₂PdCl₄ (19 mg, 0.065 mmol, 10 mol%) and P(*t*-Bu)Cy₂ (32 mg, 0.126 mmol, 20 mol%) were loaded into a Schlenk bomb fitted with a screw-top Teflon cap and suspended in ~10 mL of NH(*i*-Pr)₂. The Schlenk bomb was sealed and brought outside of the glovebox, the Teflon cap was replaced with a rubber septum under positive N₂ pressure, and 1-iodo-2-methylbenzene was injected *via* syringe (80 μL, 0.628 mmol, 1 equiv.). The rubber septum was removed under positive N₂ pressure, the Schlenk bomb was resealed, and the reaction mixture was placed in an oil bath at 80 °C for 20 min (for activation), affording a pale-yellow solution. The Schlenk bomb was brought back inside the glovebox and tetramethylammonium fluoride (TMAF) (293 mg, 3.15 mmol, 5 equiv.) was added followed by [PN]-CCPh (**3**) (250 mg, 0.629 mmol, 1 equiv.). The contents of the Schlenk bomb were brought back outside the glovebox and heated at 120 °C. Over the next 96 h, the reaction mixture grew increasingly orange, but its appearance was obscured by a large amount of grey precipitate. The reaction mixture was then concentrated under vacuum at 80 °C to remove the relatively high boiling amine solvent. The residual non-volatiles were extracted with 10 mL of pentane and filtered through a silica plug. The plug was washed with an additional 25 mL of pentane and the filtrate was concentrated under vacuum, affording a clear oil (33 mg, 0.172 mmol, 27%). The purity of Ph-C≡C-(*o*-Tol) was confirmed by ¹H and ¹³C{¹H} NMR spectroscopy.⁵¹

DFT calculations, electrochemistry, and X-ray crystallography

See the ESI† for details.

Conflicts of interest

There are no conflicts to declare.

Acknowledgements

M.F.C. thanks the University of Hawai'i at Mānoa (UHM) for generous start-up funds and laboratory space and the National Science Foundation (NSF) for a CAREER Award (NSF CHE-1847711). Mass spectroscopic data was obtained at UHM on an Agilent 6545 Accurate-Mass QTOF-LCMS (NSF-1532310). C.H.G. is grateful for undergraduate funding through the UROP program at UHM. C.E.K thanks Gaël Ung (UConn) for his assistance with electrochemical experiments. R.P.H. thanks Dartmouth College for access to computational resources. Elemental analyses were conducted by William Brennessel (University of Rochester).

Notes and references

- For a historical perspective: C. C. C. J. Seechurn, M. O. Kitching, T. J. Colacot and V. Snieckus, *Angew. Chem., Int. Ed.*, 2012, **51**, 5062–5085.
- (a) A. F. Littke and G. C. Fu, *Angew. Chem., Int. Ed.*, 2002, **41**, 4176–4211; (b) R. Martin and S. L. Buchwald, *Acc. Chem. Res.*, 2008, **41**, 1461–1473.
- D. A. Culkin and J. F. Hartwig, *Organometallics*, 2004, **23**, 3398–3416.
- (a) V. V. Grushin and W. J. Marshall, *J. Am. Chem. Soc.*, 2006, **128**, 12644–12645; (b) E. J. Cho, T. D. Senecal, T. Kinzel, Y. Zhang, D. A. Watson and S. L. Buchwald, *Science*, 2010, **325**, 1679–1681; (c) M. C. Nielsen, K. J. Bonney and F. Schoenebeck, *Angew. Chem., Int. Ed.*, 2014, **53**, 5903–5906; (d) D. M. Ferguson, J. R. Bour, A. J. Canty, J. W. Kampf and M. S. Sanford, *Organometallics*, 2019, **38**, 519–526.
- This was the impetus behind the merging of Pd- (or Ni-) catalyzed cross-coupling with photoredox catalysis: (a) J. C. Tellis, C. B. Kelly, D. N. Primer, M. Jouffroy, N. R. Patel and G. A. Molander, *Acc. Chem. Res.*, 2016, **49**, 1429–1439; (b) J. Twitlon, C. Le, P. Zhang, M. H. Shaw, R. W. Evans and D. W. C. MacMillan, *Nat. Rev.*, 2017, **1**, 0052.
- (a) M. M. Heravi and L. Mohammadkhani, *J. Organomet. Chem.*, 2018, **869**, 106–200; (b) See ref. 2b.
- D. Milstein and J. K. Stille, *J. Am. Chem. Soc.*, 1978, **100**, 3636–3638.
- C. Cordovilla, C. Bartolome, J. M. Martinez-Iharduya and P. Espinet, *ACS Catal.*, 2015, **5**, 3040–3053.
- (a) Ref. 8 (b) P. Stanetty, M. Schnürch and M. D. Mihovilovic, *J. Org. Chem.*, 2006, **71**, 3754–3761; (c) M. Zhang, X. Guo and Y. Li, *Macromolecules*, 2011, **44**, 8798–8804.
- (a) L. A. Agrofoglio, I. Gillaizeau and Y. Saito, *Chem. Rev.*, 2003, **103**, 1875–1916; (b) A. ElMarrouni, M. Campbell, J. J. Perkins and A. Converso, *Org. Lett.*, 2017, **19**, 3071–3074; (c) L. Wicke and J. W. Engels, *Bioconjugate Chem.*, 2012, **23**, 627–642; (d) A. Mescic, A. Harej, M. Klobucar, D. Glavac, M. Cetina, S. K. Pavelic and S. Raic-Malic, *ACS Med. Chem. Lett.*, 2015, **6**, 1150–1155.
- C. Elschenbroich, *Organometallics*, WILEY-VCH, 3rd edn, 2006.
- (a) D. Gudat, *Acc. Chem. Res.*, 2010, **43**, 1307–1316; (b) D. Gudat, *Dalton Trans.*, 2016, **45**, 5896–5907.
- S. Burck, D. Gudat, M. Nieger and J. Tirreé, *Dalton Trans.*, 2007, 1891–1897.
- (a) V. Kremláček, J. Hyvl, W. Y. Yoshida, A. Růžicka, A. L. Rheingold, J. Turek, R. P. Hughes, L. Dostál and M. F. Cain, *Organometallics*, 2018, **37**, 2481–2490; (b) J. Hyvl, W. Y. Yoshida, C. E. Moore, A. L. Rheingold and M. F. Cain, *Polyhedron*, 2018, **143**, 99–104; (c) J. Hyvl, W. Y. Yoshida, A. L. Rheingold, R. P. Hughes and M. F. Cain, *Chem. – Eur. J.*, 2016, **22**, 17562–17565.
- H. A. Bent, *Chem. Rev.*, 1961, **61**, 275–311.
- K. Sonogashira, Y. Tohda and N. Hagihara, *Tetrahedron Lett.*, 1975, **50**, 4467–4470.
- M. T. Nguyen, B. Gabidullin and G. I. Nikonov, *Dalton Trans.*, 2018, **47**, 17011–17019.
- For NMR spectra of related NHPs: S. Burck, D. Gudat, K. Nättinen, M. Nieger, M. Niemeyer and D. Schmid, *Eur. J. Inorg. Chem.*, 2007, 5112–5119.
- (a) M. Gediga, S. Burck, J. Bender, D. Förster, M. Nieger and D. Gudat, *Eur. J. Inorg. Chem.*, 2014, 1818–1825; (b) A. D. Millder, S. A. Johnson, K. A. Tupper, J. L. McBee and T. D. Tilley, *Organometallics*, 2009, **28**, 1252–1262.
- N. Tokitoh, T. Matsumoto and T. Sasamori, *Heterocycles*, 2008, **76**, 981–987.
- Additional details on the DFT calculations can be found in the ESI.†
- S. Burck, D. Förster and D. Gudat, *Chem. Commun.*, 2006, 2810–2812.
- R. Chinchilla and C. Nájera, *Chem. Rev.*, 2007, **107**, 874–922.
- P. L. Alsters, J. Boersma and G. van Koten, *Organometallics*, 1993, **12**, 1629–1638.
- (a) K. Osakada, R. Sakata and T. Yamamoto, *Organometallics*, 1997, **16**, 5354–5364; (b) K. Osakada and T. Yamamoto, *Coord. Chem. Rev.*, 2000, **198**, 379–399.
- S. Burck, D. Gudat, M. Nieger, Z. Benko, L. Nyulaszi and D. Szieberth, *Z. Anorg. Allg. Chem.*, 2009, **635**, 245–252.
- Y. Wang, Y. Chen, Z. Jiang, F. Liu, F. Liu, Y. Zhu, Y. Liang and Z. Wu, *Sci. China: Chem.*, 2019, **62**, 491–499.
- J. E. Fergusson and P. F. Heveldt, *Inorg. Chim. Acta*, 1978, **31**, 145–154.
- Y. Nishihara, H. Onodera and K. Osakada, NMR data for the related Pd complex *trans*-Pd(C₆F₅)(2,4,6-C₆F₃H₂)(PEt₃)₂, *Chem. Commun.*, 2004, 192–193.
- Related P–I species have exhibited some unusual behavior: (a) Ref. 12 (b) D. M. C. Ould, A. C. Rigby, L. C. Wilkins, S. J. Adams, J. A. Platts, S. J. A. Pope, E. Richards and R. L. Melen, *Organometallics*, 2018, **37**, 712–719; (c) G. Reeske and A. H. Cowley, *Inorg. Chem.*, 2007, **46**, 1426–1430.
- C. A. Caputo, A. L. Brazeau, Z. Hynes, J. T. Price, H. M. Tuononen and N. D. Jones, *Organometallics*, 2009, **28**, 5261–5265.

- 32 C. A. Caputo, M. C. Jennings, H. M. Tuononen and N. D. Jones, *Organometallics*, 2009, **28**, 990–1000.
- 33 M. B. Abrams, B. L. Scott and R. T. Baker, *Organometallics*, 2000, **19**, 4944–4956.
- 34 B. Pan, D. A. Evers-McGregor, M. W. Bezpalko, B. M. Foxman and C. M. Thomas, *Inorg. Chem.*, 2013, **52**, 9583–9589.
- 35 S. E. Knight, M. W. Bezpalko, B. M. Foxman and C. M. Thomas, *Inorg. Chim. Acta*, 2014, **422**, 181–187.
- 36 C. A. Tolman, *J. Am. Chem. Soc.*, 1970, **92**, 2956–2965.
- 37 N. Pirkel, A. Del Grosso, B. Mallick, A. Doppiu and L. J. Goossen, *Chem. Commun.*, 2019, **55**, 5275–5278.
- 38 K. O. Kirlikovali, E. Cho, T. J. Downard, L. Grigoryan, Z. Han, S. Hong, D. Jung, J. C. Quintana, V. Reynoso, S. Ro, Y. Shen, K. Swartz, E. Ter Sahakyan, A. I. Wixtrom, B. Yoshida, A. L. Rheingold and A. M. Spokoyny, *Dalton Trans.*, 2018, **47**, 3684–3688.
- 39 D. C. Powers and T. Ritter, *Acc. Chem. Res.*, 2012, **45**, 840–850.
- 40 (a) R. Vilar, D. M. P. Mingos and C. J. Cardin, *J. Chem. Soc., Dalton Trans.*, 1996, 4313–4314; (b) V. Dura-Vila, D. M. P. Mingos, R. Vilar, A. J. P. White and D. J. Williams, *J. Organomet. Chem.*, 2000, **600**, 198–205.
- 41 (a) F. Proutiere, E. Lyngvi, M. Aufiero, I. A. Sanhueza and F. Schoenebeck, *Organometallics*, 2014, **33**, 6879–6884; (b) M. J. Chalkley, L. M. Guard, N. Hizari, P. Hofmann, D. P. Hruszkewycz, T. J. Schmeier and M. K. Takase, *Organometallics*, 2013, **32**, 4223–4238.
- 42 W. Dai, M. J. Chalkley, G. W. Brudvig, N. Hazari, P. R. Melvin, R. Pokhrel and M. K. Takase, *Organometallics*, 2013, **32**, 5114–5127.
- 43 (a) C. Mealli, A. Ienco, A. Galindo and E. P. Carreno, *Inorg. Chem.*, 1999, **38**, 4620–4625; (b) M. A. Zhuravel, J. R. Moncarz, D. S. Glueck, K.-C. Lam and A. L. Rheingold, *Organometallics*, 2000, **19**, 3447–3454.
- 44 B. Pan, Z. Xu, M. W. Bezpalko, B. M. Foxman and C. M. Thomas, *Inorg. Chem.*, 2012, **51**, 4170–4179.
- 45 M. F. Cain, *Comments Inorg. Chem.*, 2020, **40**, 25–51.
- 46 N. Topolovcan, S. Hara, I. Cisarova, Z. Tosner and M. Kotora, The disubstituted alkyne was prepared independently via a published procedure, *Eur. J. Org. Chem.*, 2020, 234–240.
- 47 H.-J. Kim and S. W. Lee, *Bull. Korean Chem. Soc.*, 1999, **20**, 1089–1092.
- 48 N. Kakusawa, K. Yamaguchi and J. Kurita, *J. Organomet. Chem.*, 2005, **690**, 2956–2966.
- 49 A Cu(I) source is NOT always necessary: M. Gazvoda, M. Virant, B. Pinter and J. Kosmrlj, *Nat. Commun.*, 2018, **9**, 4814–4822.
- 50 M. Schilz and H. Plenio, *J. Org. Chem.*, 2012, **77**, 2798–2807.
- 51 C. W. D. Gallop, M.-T. Chen and O. Navarro, *Org. Lett.*, 2014, **16**, 3724–3727.
- 52 Y. Nakao and T. Hiyama, *Chem. Soc. Rev.*, 2011, **40**, 4893–4901.
- 53 P. M. Miura-Akagi, A. L. Rheingold and M. F. Cain, Unpublished results.